

AFRL-SR-BL-TR-98-

**REPORT DOCUMENTATION PAGE**

0667

Public Reporting burden for this collection of information is estimated to average 1 hour per response, including the time for reviewing instructions, searching existing data sources, gathering and maintaining the data needed, and completing and reviewing the collection of information. Send comment regarding this burden estimate or any other aspect of this collection of information, including suggestions for reducing this burden, to Washington Headquarters Services, Directorate for Information Operations and Reports, 1215 Jefferson Davis Highway, Suite 1204, Arlington, VA 22202-4302, and to the Office of Management and Budget, Paperwork Reduction Project (0704-0188), Washington, DC 20503.

1. AGENCY USE ONLY (Leave Blank)	2. REPORT DATE September 1998	3. REPORT TYPE AND DATES COVERED Final (15 Feb. 1995-14 Feb. 1998)
4. TITLE AND SUBTITLE Theoretical Studies of Gas Phase Elementary Reactions	5. FUNDING NUMBERS F49620-95-1-0182 2303/FS 61102F	
6. AUTHOR(S) Keiji Morokuma	8. PERFORMING ORGANIZATION REPORT NUMBER	
7. PERFORMING ORGANIZATION NAME(S) AND ADDRESS(ES) Emory University, Atlanta, GA 30322	10. SPONSORING / MONITORING AGENCY REPORT NUMBER	
9. SPONSORING / MONITORING AGENCY NAME(S) AND ADDRESS(ES) AFOSR/NL 110 Duncan Ave. Bolling AFB, DC 20332-8050		
11. SUPPLEMENTARY NOTES The views, opinions and/or findings contained in this report are those of the author(s) and should not be construed as an official Department of the Army position, policy or decision, unless so designated by the documentation.		
12 a. DISTRIBUTION / AVAILABILITY STATEMENT Approved for public release; distribution unlimited.	12 b. DISTRIBUTION CODE	
13. ABSTRACT (Maximum 200 words)		

Understanding the mechanism, kinetics and dynamics of elementary gas phase reactions is one of the major goals of chemistry. Such understanding is also essential to predicting and understanding plasma dynamics and optical radiation associated with the spacecraft-atmosphere interactions. The objective of the present research was to provide, based on mainly the ab initio molecular orbital and some dynamics calculations, theoretical information concerning the potential energy surfaces that dictate the kinetics and dynamics of gas phase elementary reactions. The reactions studied include ion-molecule reactions, photochemical reactions and neutral elementary reactions. Many of the systems for which theoretical calculations were performed in the present research are relevant to atmospheric chemistry and chemical lasers. Many systems were chosen based on the experimental studies and in collaboration with scientists at Air Force Research Laboratory, in order to provide them with some new insight that is not easily available without theoretical studies.

14. SUBJECT TERMS gas phase elementary reaction, theoretical studies		15. NUMBER OF PAGES 18
		16. PRICE CODE
17. SECURITY CLASSIFICATION OR REPORT UNCLASSIFIED	18. SECURITY CLASSIFICATION ON THIS PAGE UNCLASSIFIED	19. SECURITY CLASSIFICATION OF ABSTRACT UNCLASSIFIED
20. LIMITATION OF ABSTRACT UL		

NSN 7540-01-280-5500

Standard Form 298 (Rev. 3-89)  
Prescribed by ANSI Std. Z39-18  
298-102

Enclosure 1

## Accomplishments and New Findings.

### A. Ground and Excited State Potential Energy Surfaces of (H, C, N, O) Cation and Neutral Systems.

The chemistry of a series of chemical reactions involving species given in general formula of (H, C, N, O) and (H, C, N, O)<sup>+</sup>, which has been a focus of interest of AFOSR, has been a target of the present project.

#### A-1. Potential Energy Surfaces of the [H, C, N, O] Cation System.

In this work, the global potential energy surfaces (PESs) of the [H,C,N,O]<sup>+</sup> system both in doublet and quartet states have been rather exhaustively studied with the B3LYP density functional method, with special attention to cover nearly all intermediates and transition states. Ionization potentials, energies of reactions and proton affinities of fragments are calculated and compared with experiments for assess the reliability. In the doublet state, all six chain isomers and three cyclic structures exist, and rearrangements among them take place over high barriers mainly via 1,3-H shift and chain-cycletransformation. Pathways for fragmentations of isocyanic acid cation HCNO<sup>+</sup> and fulminic acid cation HCN<sup>+</sup> have been identified and compared with the experiments. In the quartet state, there exist ion-molecule complexes between fragments as well as trans and cis forms of chain isomers and cyclic and open branched isomers, and the potential surfaces for interconversion and fragmentation are much more complicated. The potential energy profiles for the reaction of O<sup>+</sup>(<sup>4</sup>S) + HCN have been examined and pathways for production of experimentally observed HCN<sup>+</sup>, NO<sup>+</sup>, HCO<sup>+</sup> and HOC<sup>+</sup> have been identified to go through long-lived chain intermediates HCNO<sup>+</sup> and HOCN<sup>+</sup> and open branched intermediate NCHO<sup>+</sup>, while production of CO<sup>+</sup> is more complicated. The crossing seam minimum with the doublet has been found right at the quartet intermediate HCNO<sup>+</sup>, and intersystem crossing and production of the stable doublet fulminic acid cation HCN<sup>+</sup> is likely to be an efficient process.

#### A-2. Potential Energy Surfaces of the (H, C, N, O) Neutral System.

It has been also found that the reaction of the cationic O<sup>+</sup>(<sup>4</sup>S) with HCN in the space shuttle exhaust condition can lead to some neutral products such as NH + CO. This observation indicates a possibility of crossing of the neutral and cationic [H,C,N,O] potential energy surfaces. The [H,C,N,O] decomposition reactions are relevant to the practically important RAPRENNO<sub>x</sub> process, which involves the removal of NO<sub>x</sub> combustion products by the injection of (HOCN)<sub>3</sub> into exhaust streams. The reactions of the decomposition products, such as HCN and O, CH and NO, NH and CO, OH and CN, also play important roles in the combustion of N-containing hydrocarbon fuels. While some of these reactions, in particular HNCO → NH + CO, O + HCN, CH + NO, HNCO → H + NCO, have been studied experimentally, the reaction mechanisms are not yet well understood. Reactions of O + HCN have also been studied in gas-phase single-collision conditions. Thus we have performed theoretical studies on the PESs of the neutral [H,C,N,O] system.

In this work, global PESs of the neutral [H,C,N,O] system in singlet and triplet states have been investigated using the hybrid density functional B3LYP/6-311G(d,) method. Isocyanic acid, HCHCO **1**, has been found to be the most stable isomer for both multiplicities. The adiabatic singlet-triplet splitting for **1** is 82.6 kcal/mol. In the singlet state, HNCO is energetically followed by cyanic acid. HOCN **2**, 28.7 kcal/mol higher than **1**, fulminic acid, HCNO **3** (67.9 kcal/mol), and isofulmanic acid, HONC **4** (87.1 kcal/mol). In the triplet state, the branched NC(H)O isomer <sup>3</sup>**7** is 0.3 kcal/mol higher than <sup>3</sup>**1**, followed by HOCN <sup>3</sup>**2** (27.9 kcal/mol relative to triplet HNCO and HCNO <sup>3</sup>**3** (40.6 kcal/mol). The barriers for intramolecular rearrangements within singlet and triplet [H,C,N,O] system have been calculated to be high, and the isomerization processes in most cases are not expected to compete with fragmentations. Several minima on the singlet-triplet seam of crossing, relevant to the singlet [H,C,N,O] decomposition reactions, have been also found. The global features of the singlet and triplet PES have been applied to several important reactions, such as NH(<sup>3</sup>S) + CO, thermal decomposition of HNCO, O(<sup>3</sup>P) + HCN, O(<sup>3</sup>P) + HNC, and CH(<sup>2</sup>P) + NO(<sup>2</sup>P). For these reactions, major product channels have been speculated and their activation energies have been reported. Adiabatic ionization potentials for singlet and triplet [H,C,N,O] have been found to be high, in the range of 180 – 270 kcal/mol.

#### A-3. Potential Energy Surface for Photodissociation of HNCO in the S<sub>1</sub> State.

Recent experiments conducted by the research groups of Reisler et al. and Crim et al. have investigated the photodissociation of HNCO in the first ultraviolet absorption band. Irradiation in the first absorption band accesses two spin-allowed dissociation pathways, fission of the C-N and the N-H bond, to give  $\text{HN}(a^1\Delta) + \text{CO}(X)$  and  $\text{H} + \text{NCO}(X^2\Pi)$ , respectively. Both groups of researchers believe that barriers to the two bond fission processes exist upon the surface accessed by irradiation in the first band. Much experimental work followed by theoretical work has been done on understanding the pathways of photo-excited HNCO complex. There is also a spin-forbidden channel at low energy to give  $\text{HN}(X^3\Sigma^-) + \text{CO}(X)$ .

The CASSCF geometries and MRSDCI energies agree well with the known experimental geometries and N-H and C-N dissociation energies of the HNCO molecule. The present calculations indicate that no reaction channel is open on the  $S_1$  potential surface up to around 124-5 kcal/mol. Any reaction which occurs below this energy, e. g. N-H fission experimentally observed at the threshold of 110 kcal/mol, has to come from reaction in the ground  $S_0$  state via  $S_1 \rightarrow S_0$  internal conversion, or in the  $T_1$  state via  $S_1 \rightarrow T_1$  ( $i=1,2$ ) intersystem crossing.

The MRSDCI calculations indicate that the C-N fission channel on  $S_1$  opens at around 124-5 kcal/mol. Efficient C-N fission observed experimentally above this energy range should proceed directly on  $S_1$  with only a small reverse barrier of 1-2 kcal/mol. This is consonant with the observation of an anisotropic distribution of fragments from the formation of NH and CO following excitation at 230.1 nm (124.3 kcal/mol) and with very recent experiments which find the barrier height to be approximately 1-2 kcal/mol. The calculations indicate that C-N fission near the threshold should exclusively go through the trans transition state which can be reached directly from the trans configuration, to which the initial non-vertical excitation and the early dynamics would send the system.

The calculation also shows that fission of the weaker N-H bond on  $S_1$  has a substantial barrier and cannot take place at low energies. At a higher energy of about 127-8 kcal/mol, the N-H fission pathway finally opens up. This channel at its threshold should occur exclusively via a cis transition state, which has a lower barrier and can be reached from the more populated trans configuration via the isomerization transition state open at about 120 kcal/mol. There is a substantial difference between the higher trans and the lower cis barriers for the N-H fission. These two channels might possibly be distinguished experimentally by further interrogation of the dynamics of photodissociation.

Experimental results by Crim et al. on the enhancement of N-H fission is very interesting. At the total excitation energy of 127.1 kcal/mol, supplying about 29 kcal/mol of this energy as three quanta of N-H stretch prior to UV excitation dramatically increased the OCN product yield to 83% from 21% when all the energy is supplied in UV excitation. As discussed above, the N-H fission channel on  $S_1$  has just opened up, and the geometry of the transition state **TS-CNH** suggests that the N-H stretch will help the system to reach the transition state. However, if the N-H stretch energy is locked in this mode, the system originally excited into a trans configuration would not have enough energy left to go over the isomerization barrier (at 120 kcal/mol) to reach the cis side of configuration before finding the cis transition state **TS-CNH**. The transition state for N-H fission in the trans configuration **TS-TNH** is much higher in energy (143 kcal/mol) and is not available. Several possible explanations may be conjectured. If there is a low energy (at about 100 kcal/mol) pathway connecting trans to cis configuration on the way to the N-H fission transition states, the system with a large N-H internal energy may be able to reach the cis transition state. Experimentally, if N-H fission at this energy is mainly taking place on the ground electronic state via efficient  $S_1 \rightarrow S_0$  internal conversion, the system may be able to reach the N-H fission product using the N-H stretch energy effectively.

#### A-4. Potential Energy Surfaces for Photodissociation of HNCO. $S_0$ - $S_1$ and $S_0$ - $T_1$ Seams of Crossing.

Isocyanic acid, HNCO, is an important chemical in a broad spectrum of combustion processes. The unimolecular decomposition of HNCO has been studied extensively in the recent past. Such state-of-the-art techniques as photofragment imaging have been successfully employed to study the dynamics of the system (Reisler; Crimm; Volpp). In these experiments it was found that three different channels,  $\text{HN}(^3\Sigma^-) + \text{CO}(^1\Sigma^+)$ ,  $\text{H} + \text{NCO}(^2\Pi)$ , and  $\text{HN}(^1\Delta) + \text{CO}(^1\Sigma^+)$ , compete for dissociation, and this competition is strongly dependent upon the excitation wavelength. Initial HN stretch mode-selective excitation followed photodissociation greatly enhances the production of  $\text{H} + \text{NCO}(X^2\Pi)$ .

The spin-forbidden channel at low energy to give  $\text{HN}(X^3\Sigma^-) + \text{CO}(X)$  has to take place in the  $T_1$  state via  $S_1 \rightarrow T_1$  intersystem crossing. Some reactions into the two spin-allowed channels, especially at low

excitation energy, have to take place on the ground  $S_0$  state via  $S_1 \rightarrow S_0$  internal conversion. Thus, the location of seam of  $S_1/S_0$  conical interaction or  $S_1/T_1$  crossing is very important in understanding the full reaction mechanism of HNCO photodissociation, and we are presently carrying out calculations for these seams of crossing.

In the present study, we used high level ab initio calculations, CASSCF and CASPT2, to investigate the complex processes of HNCO photodissociation dynamics, involving four distinct potential energy surfaces,  $S_0$ ,  $S_1$ ,  $T_1$  and  $T_2$ . Numerous internal conversion coupling channels and intersystem crossing were located. Results of several experimental studies are used as a guide to unravel the puzzle of competition for dissociation between three channels:  $\text{HN}({}^1\Delta) + \text{CO}$  [3],  $\text{H} + \text{NCO}({}^2\Pi)$  [2], and  $\text{HN}({}^3\Sigma^-) + \text{CO}$  [1]. The final PESs for each of the three product channels were obtained. A low reverse barrier of 1.2 kcal/mol to product [3] was confirmed to be on  $S_1$ . Rather low reverse barriers on  $T_1$  and  $T_2$  were found to block the passage to product [2]. At photoexcitation energies near channel [3] threshold, products to channel [3] are suggested to be yielded via the following mechanisms:

$S_1 \rightarrow [3]$  (if enough energy in excitation) and  $S_1 \rightarrow S_0 \rightarrow [3]$

Channel [2] mechanism is substantially more complicated:

$S_1 \rightarrow S_0 \rightarrow [2]$ ;  $(\text{HN quanta}) + S_1 \rightarrow T_1 \rightarrow [2]$ ;  $S_1 \rightarrow T_2 \rightarrow [2]$ ;  $S_1 \rightarrow T_2 \rightarrow T_1 \rightarrow [2]$

And finally, the system is suggested to dissociate into channel [1] as follows:

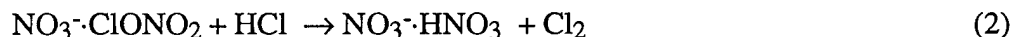
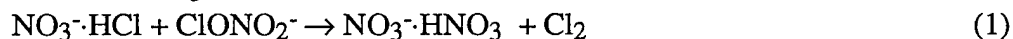
$S_1 \rightarrow S_0 \rightarrow T_1 \rightarrow [1]$  and  $S_1 \rightarrow T_1 \rightarrow [1]$ .

At higher photoexcitation energies channel [3] is expected to be dominant while channel [2] is expected to drop rapidly. Products of channel [1] are expected to appear at any excitation wavelength.

## B. Potential Energy Surfaces for Ion-Molecule Reactions.

### B-1. Ab Initio and Density Functional Study of the Reaction of HCl with ClONO<sub>2</sub> Catalyzed by NO<sub>3</sub><sup>-</sup>.

Al Viggiano and Robert Morris of Phillips Lab, Hanscom AFB recently published a communication (J. M. Van Doren, A. A. Viggiano and R. A. Morris, J. Am. Chem. Soc., **116**, 6957 (1994)), in which they have reported that the reaction of HCl with ClONO<sub>2</sub> is accelerated strongly when one or the other reactant is clustered with an NO<sub>3</sub><sup>-</sup> ion.



However, neither the origin of this enhancement nor the detailed mechanism of these reactions is not well understood. Thus, Dr. Alexander Mebel in part supported by this grant and PI have studied the potential energy surface for the reaction of HCl with ClONO<sub>2</sub> in the presence of NO<sub>3</sub><sup>-</sup> using ab initio (MP2) and density functional (B3LYP) methods. All the structures of the reactants, intermediates and transition states are optimized.

The  $\text{HCl} + \text{ClONO}_2 \rightarrow \text{Cl}_2 + \text{HONO}_2$  reaction without NO<sub>3</sub><sup>-</sup> is shown to have a high barrier of 45-64 kcal/mol. The NO<sub>3</sub><sup>-</sup> ion catalyzes the reaction and here three different mechanisms are possible. In the stepwise mechanism, HCl reacts first with NO<sub>3</sub><sup>-</sup> to form the Cl<sup>-</sup>·HNO<sub>3</sub> complex which then dissociates to Cl<sup>-</sup> and HNO<sub>3</sub>,



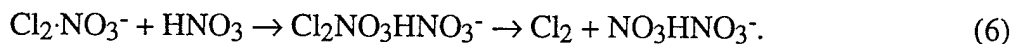
In the second step, Cl<sup>-</sup> attacks ClONO<sub>2</sub> to produce Cl<sub>2</sub>·NO<sub>3</sub><sup>-</sup> decomposing to Cl<sub>2</sub> and NO<sub>3</sub><sup>-</sup>,



The reactions (3) and (4) occur without barrier and the activation energy of the stepwise mechanism is nothing but the exothermicity of the reaction (4), 8.9 and 10.4 kcal/mol at the B3LYP/6-31+G(d) and MP2/6-31+G(d) levels, respectively, which is close to the experimental value of 8.8 kcal/mol. In the concerted mechanism I, the reaction (3) is followed by the association of Cl<sup>-</sup>·HNO<sub>3</sub> with ClONO<sub>2</sub> giving the NO<sub>3</sub>ClClHNO<sub>3</sub><sup>-</sup> complex **III.1** which decomposes to Cl<sub>2</sub>·NO<sub>3</sub><sup>-</sup> + HNO<sub>3</sub>,

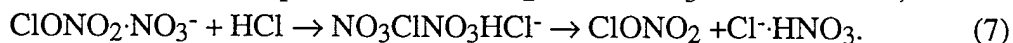


Cl<sub>2</sub>·NO<sub>3</sub><sup>-</sup> can either dissociate to Cl<sub>2</sub> + NO<sub>3</sub><sup>-</sup> or form with HNO<sub>3</sub> the Cl<sub>2</sub>NO<sub>3</sub>HNO<sub>3</sub><sup>-</sup> complex **III.8**. The latter decomposes to Cl<sub>2</sub> and NO<sub>3</sub>HNO<sub>3</sub><sup>-</sup>,



All the steps of the concerted mechanism I have no barrier, and the reaction occurs with a negative activation energy and with the overall exothermicity of 43.4 and 38.4 kcal/mol at the B3LYP and MP2 levels, respectively.

If the  $\text{ClONO}_2 \cdot \text{NO}_3^-$  is formed, it reacts with  $\text{HCl}$ , but  $\text{Cl}_2 + \text{NO}_3\text{HNO}_3^-$  cannot be produced directly. Instead, the reaction proceeds by the concerted mechanism II, starting with formation of the  $\text{NO}_3\text{ClONO}_2\text{HCl}^-$  complex **III.2** and its decomposition to  $\text{ClONO}_2 + \text{Cl} \cdot \text{HNO}_3$  without barrier,



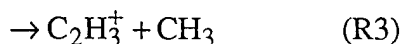
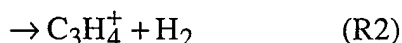
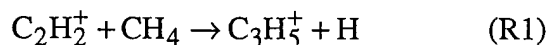
In the next step, the concerted mechanism II merges with the concerted mechanism I and the reactions (5) and (6) take place. At low temperatures, the  $\text{HCl} + \text{ClONO}_2 + \text{NO}_3^-$  reaction is predicted to occur by the concerted mechanisms I and II and to exhibit a negative temperature dependence for the rate coefficient.

### B-2. The Mechanism of $\text{C}_2\text{H}_2^+ + \text{NH}_3$ Reaction. Efficient Charge Transfer and Proton Transfer Processes Competing with Stable Complex Formation.

High level *ab initio* calculations have been performed to investigate the mechanism of the ion-molecule reaction  $\text{NH}_3 + \text{C}_2\text{H}_2^+$ . Three channels, covalent complex formation (CC), proton transfer (PT) and charge transfer (CT), have been studied. Among the two pathways found for the PT channel, one leads the reactants  $\text{NH}_3 + \text{C}_2\text{H}_2^+$  to  $\text{NH}_4^+ + \text{C}_2\text{H}({}^2\Pi)$  through a moderately bound complex without any barrier, and the other leads  $\text{NH}_3 + \text{C}_2\text{H}_2$  to the H-atom transferred products  $\text{NH}_4^+ + \text{C}_2\text{H}({}^2\Sigma^+)$  with a modest barrier. These findings support the fast "stripping" mechanism proposed by Anderson et al. As to the CC channel, several isomers of  $\text{C}_2\text{H}_5\text{N}^+$  and the isomerization transition states have been located. No significant barrier relative to the reactants have been found on either the ground or the  ${}^2A''$  excited state. To rationalize the experimental fact that no CC channel products have been observed, it is argued that the reactants  $\text{NH}_3 + \text{C}_2\text{H}_2^+$  correlate adiabatically to excited states of covalent  $\text{C}_2\text{H}_5\text{N}^+$  species, whose formation requires significant alternation of the  $\text{C}_2\text{H}_2^+$  geometry and electronic structure. Therefore, the system is most likely to follow the PT or the CT channel instead of visiting the CC channel. For the CT channel, limited potential energy surface (PES) scans of the three electronic states ( $1,2 {}^2A' + {}^2A''$ ) indicate that CT at different approach angles or between electronic states of different symmetries ( $A' \rightarrow A'$ ,  $A'' \rightarrow A'$ ) may produce final products of different characteristics, and might account for the two pathways proposed by Anderson et al.

### B-3. The Mechanism of $\text{C}_2\text{H}_2^+ + \text{CH}_4$ Reaction. Mode-Enhancement Effect.

Controlling the outcome of a chemical reaction is the dream of chemists and a fascinating branch of modern chemistry. The mode-selective chemistry, controlling photodissociation process of vibrationally or rovibrationally selected small molecules. Applications to polyatomic bimolecular reactions have been limited due to the difficulty of preparing mode-selective excited reactants and quick relaxation of selected vibrational excitations. However Zare et al. recently studied the reaction of ammonium ion and  $\text{ND}_3$ , and found that the umbrella mode of  $\text{NH}_3^+$  enhances charge transfer and deuterium abstraction significantly, while the isoenergetic excitation of the breathing mode does not induce any effect. In another experiment, Anderson et al. have studied the effects of collision energy and mode-selective vibrational excitation on the reaction of  $\text{C}_2\text{H}_2^+$  with  $\text{CH}_4$  and  $\text{CD}_4$ . Two distinct reaction mechanisms are active in the energy range below 5 eV. At low energies, a long-lived  $\text{C}_3\text{H}_6^+$  complex forms efficiently and then decomposes primarily to  $\text{C}_3\text{H}_5^+ + \text{H}$  and  $\text{C}_3\text{H}_4^+ + \text{H}_2$ . (R1, R2)



Competing with R1 and R2 is a hydrogen transfer reaction R3, producing  $\text{C}_2\text{H}_3^+ + \text{CH}_3$  with little atom scrambling. The R3 channel is strongly enhanced by collision energy and becomes dominant above 0.4 eV. One interesting feature of this channel is that two quanta of a C-H bending modes ( $\sim 155 \text{ meV}$ ) enhance the reaction at least  $\sim 10$  times! Based on the isotope study with  $\text{CD}_4$ , they concluded that there exist two possible reaction mechanisms for R3:  $\text{CH}_3$  elimination from a long-lived  $\text{C}_3\text{H}_6^+$  complex and a direct H-atom abstraction through an intermediate, where the latter path is dominant by a factor of 5~10:1. They also

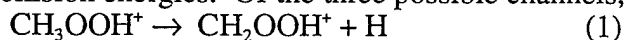
predicted an early barrier of about  $150 \pm 50 \text{ meV}$ . The enhancement effect of C-H bending excitation on the reaction rate is explained by the necessity of carbon atom rehybridization from  $sp$  to  $sp^2$  to reach a bent transition state during the process.

We have performed high level ab initio calculations to investigate the mechanism of the ion-molecule reaction of  $\text{CH}_4 + \text{C}_2\text{H}_2^+$ . Compared to the previous work of Klippenstein, a very similar profile of the H-abstraction channel (R3) is obtained despite some subtle differences. No entrance or exit barrier was found, and the reaction proceeds through a moderately bound ( $\sim 15 \text{ kcal/mol}$ ) intermediate complex. For the complex channel (R1, R2), a new transition state, **com\_TS1**, with a  $C_1$  structure has been located. The geometry and energetics of this structure seem to be more consistent with experimental findings, and it is expected that a qualitatively correct cross section can be derived using the results in the current work.

Our initial attempt at direct trajectory calculation in the current system is not very satisfactory, since no reactive events have been found. Nevertheless, we do notice that asymmetric H-C-C bending participates in the reaction actively, and nearly induced reaction in one of the trajectory we have propagated. Clearly, one has to choose the initial conditions wisely to gain any insights into the reaction process due to the limited number of calculations that one can afford in direct trajectory study.

#### B-4. Reactions of $\text{O}_2^+ + \text{CH}_4$ .

This reaction has attracted a substantial attention from the viewpoint of chemistry in the stratosphere and  $\text{CH}_4/\text{O}_2$  combustion flames. Many experimental studies, including some from the Air Force Research Laboratory, have been carried out on this reaction (S. E. Barlow, E. E. Ferguson, et al, J. Chem. Phys. 85, 385 (1986); A. A. Viggiano, R. A. Morris, J. M. Van Doren, and J.F. Paulson, J. Chem. Phys. 96, 275 (1992)), providing detailed knowledge about the rate constants and reaction dynamics over a wide range of translational collision energies. Of the three possible channels,



(1) is the only process observed experimentally at thermal energy. Based on experimental results, it was suggested that initially a weak outer complex is formed prior to C-H insertion.

We have performed potential energy surface calculation for this system at various levels of theory. This outer complex was indeed found to be bound at all levels of theory with H-O distances ranging between 2.6 and 2.8 Å. The stabilization of this complex amounts to about 11 kcal/mol with both density functional and MP2 methods, in reasonable agreement with 9 kcal/mol as proposed by Barlow et al. G2 type calculations do not change the energetics too much. The  $\text{H}-\eta^2$  complex with  $\text{O}_2^+$  bound side-on was predicted to be the most stable among the many possible conformations. The first compound to be expected after the  $\text{O}_2^+$  attack is the vibrationally excited methyl hydroperoxide cation, which subsequently relaxes by H atom abstraction. The energetics of these channels have been studied and the endothermicity of the latter two reaction products as well as the stabilization of the products of (1), approx. 25 kcal/mol, could be reproduced by our calculations.

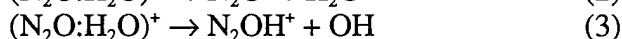
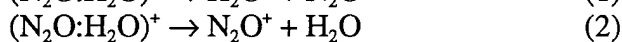
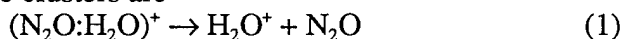
#### B-5. Reaction of Methanol Cation + $\text{C}_2\text{H}_2$ .

The study of this reaction was initiated due to its importance in experimental research in the Air Force Research Laboratory. Unfortunately these experiments turned out to be difficult and the experimental project has since been abandoned. Nevertheless, the reaction remains nevertheless interesting due to its similarities and differences with the experimentally accessible reactions  $\text{C}_2\text{H}_2^+ + \text{NH}_3$  and  $\text{C}_2\text{H}_2^+ + \text{CH}_4$ . There are three main reaction channels common to these reactions: complex formation (CF), charge transfer (CT) and proton transfer (PT), while channel CF was only observed experimentally in the reaction with methane. The reason for this difference was attributed to the fact that the electronic state of the reactants correlates with excited states of the complex with molecular structure very different from that of the ground state reactants. It will be interesting to see if this finding can be corroborated by our calculations on the reaction with the water cation. In addition, it is hoped that systematic trends may be detected due to the increase in electronegativity in the series  $\text{CH}_4$ ,  $\text{NH}_3$ , and  $\text{OH}_2$ . Although, a number of ab initio investigations exists for the products of the complex formation channel, such as the cations of acetaldehyde, vinyl alcohol, or hydroxy(methyl)carbene, there are no theoretical calculations in the literature which deal with the  $\text{C}_2\text{H}_2 + \text{H}_2\text{O}^+$  or  $\text{CH}_3\text{OH}^+$  reaction.

In order to elucidate the mechanics of this reaction we carried out full geometry optimizations at the B3LYP/SVP level of theory, followed by G2M energy evaluations for the stationary points on the potential energy surfaces. As usual, frequency calculations were carried out for a characterization of these structures. In addition, the MSX (minimum on the seam of crossing) for a transition from A' to A'' states was located in the vicinity of the products.

#### B-6. Structure, Spectroscopy and Reaction of $(\text{N}_2\text{O}:\text{H}_2\text{O})^+$ Cation Cluster.

Recent work by Dressler and coworkers at the Air Force Research Laboratory (M.J. Bastain, R.A. Dressler, D.J. Lavandier, E. Murad, F. Muntean and P.B. Armentrout, *J. Chem. Phys.* 106, 9570 (1997)) has experimentally probed the  $(\text{N}_2\text{O}:\text{H}_2\text{O})^+$  cluster cation with photodissociation experiments and collision induced dissociation experiments. The ion complex is created via ionization of  $\text{N}_2\text{O}$  and  $\text{H}_2\text{O}$  supersonic beam and then irradiated at frequencies of 15,000-24,000  $\text{cm}^{-1}$  in the photodissociation experiments, while the collision experiments with inert gases probe the cluster with impact energies of up to 2 eV. The observed reactions of the clusters are



In the collision induced dissociation, reaction (1) is by far predominant, while (2) and (3) are minor channels. In photodissociation, (2) is predominant, though (1) is competitive, and (3) is a very minor reaction. Bowers et al. (S.T. Graul, H-S. Kim and M.T. Bowers, *Int. J. Mass Spectrom. Ion Proc.* 117, 507 (1992)) obtained similar qualitative results in photodissociation experiments and suggest that excitation for photodissociation occurs from two stable cluster complexes, one of the type  $(\text{N}_2\text{O}^+:\text{H}_2\text{O})$  and the other of the type  $(\text{N}_2\text{OH}^+:\text{OH})$ . Some preliminary ab initio calculations supported this. However Bastian et al. interpret the results of their experiments as evidence for the existence of only one  $(\text{N}_2\text{O}:\text{H}_2\text{O})$  isomer.

The ground state PES of the  $(\text{N}_2\text{O}:\text{H}_2\text{O})^+$  cation cluster was explored with ab initio molecular orbital theory. B3LYP optimizations are used to determine the structure of the cluster and the dissociation products as well as the transition states that connect the various stable cluster ion minima. Energetics for all optimized structures are determined with the G2M(RCC,MP2) method. The results are used to interpret collision-induced dissociation (CID) experiments which study the cluster ion, and which find that the cluster dissociates to form  $\text{H}_2\text{O}^+ + \text{N}_2\text{O}$ ,  $\text{N}_2\text{OH}^+ + \text{OH}$ , and  $\text{N}_2\text{O}^+ + \text{H}_2\text{O}$  products. The calculations on a  $(\text{N}_2\text{O}^+:\text{OH}_2)^+$  complex as well as a similar  $(\text{H}_2\text{O}:\text{N}_2\text{O})^+$  complex, and show that these complexes access the experimentally observed  $\text{H}_2\text{O}^+ + \text{N}_2\text{O}$  products and  $\text{N}_2\text{OH}^+ + \text{OH}$  products without any intervening reverse barrier. The stability of both these complexes, approximately -20 kcal/mol relative to the  $\text{H}_2\text{O}^+ + \text{N}_2\text{O}$  products, agrees well with experimentally determined CID thresholds for all products. Additional calculations of the ground state potential energy surface of the cluster investigate the possibility of the formation of other products. Some preliminary studies of the excited states of the cluster cation are also performed. The results of these calculations lend insight into experimental photodissociation studies of the cluster ions, and mechanisms for the formation of  $\text{H}_2\text{O}^+ + \text{N}_2\text{O}$ ,  $\text{N}_2\text{OH}^+ + \text{OH}$ , and  $\text{N}_2\text{O}^+ + \text{H}_2\text{O}$  products following photoexcitation of the cluster ions are discussed; the  $\text{H}_2\text{O}^+ + \text{N}_2\text{O}$  and  $\text{N}_2\text{OH}^+ + \text{OH}$  products must be formed from a surface-hopping from an excited electronic state to states which correlate to ground state products. Similarly,  $\text{N}_2\text{O}^+ + \text{H}_2\text{O}$  products may be formed from collision induced dissociation of clusters only by means of a surface-hopping mechanism.

#### B-7. Potential Energy Surfaces of $\text{O}^+(^4\text{S}) + \text{H}_2\text{O}$ Charge Transfer Reaction

The calculation of the global potential energy surfaces (PESs) of the  $(\text{O}:\text{H}_2\text{O})^+$  supermolecule system relevant to the  $\text{O}^+ + \text{H}_2\text{O} \rightarrow \text{H}_2\text{O}^+ + \text{O}$  charge transfer reaction, experimentally studied at the Phillips Laboratory, has continued from the last report. Because of a large demand of computer time, which we rely much on the time allocation at the Pittsburgh Supercomputer Center, the progress has been slow for accumulating many potential energy points in six (or four if OH distances are frozen) degrees of freedom. Computations have been completed for the planar geometries, in which  $R$ ,  $\theta$  and  $\alpha$  are varied while  $\phi=0$ . More calculations have been done in which  $R$  and  $\alpha$  are varied for  $\theta=90^\circ$  and  $\phi=90^\circ$ ; at these geometries, the supermolecule has  $C_s$  symmetry. Some points have been accumulated for  $C_1$  geometries, which is extremely time-consuming. We will have to continue this painful data collection procedure another year or so.

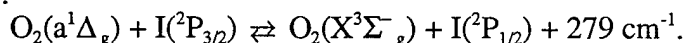


We have tried various diabatization schemes, with some success. Once enough points are accumulated, we will diabatize the adiabatic potential energy surfaces and fit the diabatic surfaces and their coupling elements to analytical functions. The fitted analytical functions will be used to run quantum and semi-classical dynamics calculations.

### C. Potential Energy Surfaces for Photochemical Reactions.

#### C-1. Ab initio Potential Energy Surfaces for the $I(^2P_{3/2}) + O_2(a^1\Delta_g) \rightleftharpoons I(^2P_{1/2}) + O_2(X^3\Sigma^-_g)$ Energy Transfer Process for Chemical Laser System.

Chemical oxygen-iodine laser (COIL) operates on spin-orbit transition of atomic iodine  $I(^2P_{1/2}) \rightarrow I(^2P_{3/2})$  at  $1.3\mu$ . The process of preparing this transition is the focus of this study. One of the several ways to produce the spin-orbit excited iodine is by electronic energy transfer induced by collisions. For instance, molecular excited state oxygen can transfer its energy to populate the spin-orbit excited levels of I, in the reaction:



We studied the pathway of this collision reaction, that is, the states involved and the geometries and energetics where transition takes place. Potential energy surfaces for all states associated with the reactants and products were obtained using CASSCF and CASPT2 methods. The spin-orbit interaction is calculated with spin-orbit CI to diagonalize the one-electron Breit-Pauli operator. Surfaces correlating with the above reactants and products were all found to be non-bonding. Shallow van der Waals minima were predicted at long range. The most favorable geometry for this transition process is non-collinear, with  $r(OO)=2.287$  bohr,  $R(M-I)=7.0$  bohr and  $\gamma=50^\circ$  in the Jacobi coordinate system, and that five adiabatic spin-orbit states are strongly involved in the process. The energies of the relevant states at the most favorable geometry are such that the crossing occurs energetically below the entrance channel  $I(^2P_{3/2})+O_2(a^1\Delta_g)$  asymptote but above the exit channel limit. This suggests that the energy transfer process should be very efficient and the quantum yield of the reaction should be high. Additional calculations are being carried out to complete this study. It is probable that these crossings are responsible for the efficient transfer of electronic energy in this system.

#### C-2. Ab Initio MO Study of the Photochemical Dissociation of Methylamine

In this work the threshold photochemistry of methylamine along three dissociation channels is examined using CASSCF and MRSDCI wavefunctions. Excitation of a nitrogen lone pair electron into a Rydberg s orbital produces an excited state that can decompose via NH rupture, CN rupture, or CH rupture. In the case of NH and CN rupture the excited state and ground state surfaces cross as the molecule dissociates forming a conical intersection. The NH rupture excited state products lie above the excitation energy and so dissociating molecules are funneled through the conical intersection and emerge as ground state products. The CN rupture excited state products lie below the excitation energy and dissociation would proceed mostly on the excited state surface. In the case of CH rupture, the excited state products lie above the excitation energy but since there is no conical intersection in this channel, CH rupture has to occur only after internal conversion to the ground state. These three mechanisms are all consistent with recent experimental evidence.

#### C-3. Potential Energy Surfaces for Photodissociation of $CX_3Y$ ( $X=H,F$ ; $Y=O,S$ ) Radicals.

The methoxy family radicals,  $CX_3Y$  ( $X=H,F$ ;  $Y=O,S$ ) are very interesting from several perspectives. They are known to be important intermediates of several combustion and atmospheric reactions. Their ground states have  $C_{3v}$  symmetry, thus subject to competitive J-T distortion and spin-orbit coupling interaction. Even though there are numerous experimental studies on those radicals, theoretical studies are very limited for the systems, especially for the excited states.

We have carried out ab initio calculations for the photodissociation of the methoxy family of radicals  $CX_3Y$  ( $X=H,F$ ;  $Y=O,S$ ) from the  $\tilde{A}^2A_1$  state. The methods employed include full valence CASSCF (for  $CH_3Y$ ), EOM-IP, EOM-CC and QRHF-CC. Optimization and normal mode analysis were done with double zeta plus polarization quality basis set, and single point energetics are done with triple zeta plus polarization quality basis. Relevant minima, transition states, and MSX (minimum on the seam of crossing) were optimized with analytical gradient. Three channels are considered: (1) predissociation to  $CX_3 + Y$ , (2) isomerization to  $CX_2-YX$  followed by dissociation to  $CX_2 + YX$ , and (3) dissociation of X. Interestingly,



different radicals represent different preferred channels. The results are summarized in Figure 3. For  $\text{CH}_3\text{O}$ , predissociation is expected to be dominant, while channel (2) opens at higher energy. H dissociation does not take place on the  $^2\text{A}_1$  excited state. For  $\text{CH}_3\text{S}$ , predissociation is expected to be dominant in all the energy range lower than  $\text{CH}_3+\text{S}(^1\text{D})$ . For  $\text{CF}_3\text{O}$ , with a much strongly bound  $\tilde{\text{A}}^2\text{A}_1$  state, the predissociation threshold over the  $^2\text{A}_1$  minimum shifts to higher energy, compared to  $\text{CH}_3\text{O}$ . The F dissociation with a low barrier of 0.62eV is likely to compete favorably with predissociation, for which the lowest MSX is 1.41eV. The branching ratio is likely to depend on the initial internal energy in the excited state. For  $\text{CF}_3\text{S}$ , the predissociation is expected to have a low threshold over the  $^2\text{A}_1$  minimum and to be efficient without competition.

Our results explain the recent experimental results of Neumark ( $\text{CH}_3\text{O}$ ) and Miller ( $\text{CF}_3\text{S}$  etc.) rather well. The fact that F dissociation is competitive with pre-dissociation might stimulate more experimental work. Further interests would be a more quantitative understanding of the process. Thus, we plan to carry out some quantum dynamics study on the pre-dissociation channel with a 2/3-D model surface and relevant spin-orbit coupling element.

#### C-4. Potential Energy Surfaces for Photodissociation of trans-Azomethane.

The mechanism of photodissociation of trans-azomethane ( $\text{CH}_3\text{-N=N-CH}_3 \rightarrow 2\text{CH}_3^\bullet + \text{N}_2$ ) has been investigated with high level ab initio molecular orbital calculations. PESs of the low-lying electronic states were explored by state-average CASSCF and MRCISD methods. The calculated vertical excitation energies for  $\text{S}_0 \rightarrow \text{S}_1$  and  $\text{S}_0 \rightarrow \text{T}_1$  transitions are in good agreement with experiments. The lowest crossing point between the  $\text{S}_0$  and  $\text{S}_1$  surfaces, around which excited molecules would make efficient internal conversion to the ground state, is found to be asymmetrical with a CNNC dihedral angle of  $92.8^\circ$  and two CNN angles of  $132.0$  and  $115.6^\circ$ , respectively. Transition structures for both simultaneous and sequential C-N bond cleavages on the  $\text{S}_0$  surface were found. Though the activation energy of sequential C-N bond cleavage is about 7 kcal/mol higher than that of the simultaneous C-N bond cleavage, the Gibbs free energy of activation is lower above  $0^\circ\text{C}$ , indicating that thermal decomposition of trans-azomethane is sequential. Photodissociation is expected to take place sequentially as well. In the sequential mechanism, dissociation of the first C-N bond on the  $\text{S}_0$  surface takes place endoergically without reverse barrier resulting in  $\text{CH}_3\text{N}_2$  intermediate, which should decompose almost immediately over a barrier of less than 1 kcal/mol. Thus the photodissociation reaction is highly asynchronous but is nearly concerted. This mechanism can explain two seemingly contradictory photodissociation experiments that two methyl radicals have very different translational as well as internal energies and that the velocity vectors of the three fragments are strongly correlated.

#### C-5. Potential Energy Surfaces for Photodissociation of ICN and $\text{CH}_3\text{I}$ .

ICN photochemical reaction in liquid Ar has been studied theoretically based on molecular dynamics simulation. The interaction potential functions between Ar and ICN in excited states as well as in the ground state were newly developed from ab initio calculation. Three types of reactions have been found for photodissociation starting from the  $^3\Pi_{0+}$  state, i.e. (i) a substantial fraction of ballistic dissociation to give mostly  $\text{I}^*(^2\text{P}_{1/2}) + \text{CN}$ , (ii) isomerization to INC, an isomer of ICN, and (iii) recombination to ICN. In the last two types of reactions, it has been found that non-adiabatic transition takes place repeatedly in the cage.

The full nine-dimensional PESs of the  $^3\text{Q}_0$  and  $^1\text{Q}_1$  states of  $\text{CH}_3\text{I}$  have been calculated with the ab initio contracted spin-orbit configuration interaction method. The results are fitted to three diabatic potential terms and their couplings as functions of all the internal degrees of freedom. The transition dipole at the Franck-Condon region has been also calculated. Surface hopping quasi-classical trajectory calculations on these potential energy surfaces have been performed to examine the photodissociation dynamics of both  $\text{CH}_3\text{I}$  and  $\text{CD}_3\text{I}$  in the A-continuum. The results are in general in good agreement with the recent experimental findings. The reasonable  $\text{I}^*/(\text{I}^*+\text{I})$ -channel branching ratio can be obtained with the PESs when the contribution of direct transition to the  $^1\text{Q}_1$  state is considered. The rotational distribution of the  $\text{CH}_3$  and  $\text{CD}_3$  fragments and its  $\text{I}^*/(\text{I}^*+\text{I})$ -channel selectivity are determined by the shape of the PESs with respect to the bending angle outside the conical intersection region. The vibrational distribution of umbrella mode is closely related to the shape of PESs for the umbrella angle; the sudden switch of reaction coordinate from  $^3\text{Q}_0$

to  $^1Q_1$  at the conical intersection is the origin of vibrational excitation in the  $I^*$  channel. The larger umbrella excitation of the  $CD_3$  fragment in both  $I$  and  $I^*$  channels, in comparison with the  $CH_3$  fragment, is related to the larger separation of the reaction coordinate from the Franck-Condon geometry. The symmetric stretching energy increases during the dissociation, which is related to the shape of PESs with respect to this coordinate, and the excitation of symmetric stretching mode seems to be possible.

### C-6. Potential Energy Surfaces for Photodissociation of Acetylene.

Even though there are large number of spectroscopic studies on  $C_2H_2$ , there are many interesting features of this simple molecule that are not yet answered. In this project, we try to answer two of them involving non-adiabatic processes. The first one arises from experimental studies of Wittig et al. They found that at 193.3nm, the dominant product of C-H fission is  $C_2H(^2\Sigma) + H(^2S)$ , which is surprising because the  $S_1$  state of  $C_2H_2$  correlates to  $C_2H(^2\Pi)+H(^2S)$ . More interestingly, when the C-H stretch modes are first populated before a 248nm UV, i.e. with a  $1200\text{cm}^{-1}$  higher total energy, the major product of the C-H fission is indeed  $C_2H(^2\Pi)+H(^2S)$ . Obviously, a non-adiabatic channel is involved. The second issue concerns the identity of the triplet perturber of the  $S_1$  state of  $C_2H_2$ . Many experimental and theoretical works have been carried out, yet the answer has not been clarified.

We have carried out *ab initio* MO calculations at the EOM-CCSD and CASSCF level for several low lying electronic states of  $C_2H_2$ . Minima, related transition states and MSX are located. Spin-orbit coupling elements are calculated at the crossing geometries. We summarize our findings as the following:

(i). A non-adiabatic photodissociation channel exists. It involves  $S_1/S_2$  transition followed by a  $S_2/S_0$  surface crossing. The highest point on this path, the dissociation TS on the  $S_2$  surface is lower than that on  $S_1$ , the highest point on the adiabatic dissociation. Thus in the 193.3nm experiment, where the photon energy is lower than the  $S_1$  dissociation TS, the non-adiabatic channel is preferred and the ground state  $^2\Sigma C_2H$  is produced. A new experiment has been suggested with specific initial mode excitation in the HCC bending mode, which might favor the non-adiabatic channel.

(ii).  $S_1$  and  $T_1$  cross at a  $C_2$  geometry within the photon energy range. However, the  $S_1$ - $T_1$  interaction is weak due to the small spin-orbit coupling.  $S_1$  and  $T_3$  also cross at a  $C_2$  geometry, and the spin-orbit coupling is an order of magnitude larger than that between  $S_1$  and  $T_1$ . The energy of this crossing is in close agreement with the energy at which anomalous ZAC spectrum was observed by Field et al. Thus, we propose that  $T_3$  is the perturber of the  $S_1$  state.

### C-7. Photodissociation of Acetylene -- Mechanism involving Triplet States.

For a small molecule, the electronic structure of  $C_2H_2$  is extremely complicated especially for the excited electronic states. The detailed mechanism of photodissociation of  $C_2H_2$  from  $S_1$  state is one of the frequently discussed issues. Basically, there are two possible non-adiabatic pathways: the path that involves transitions between singlet states, and the path involving spin-forbidden transition between  $S_1$  and close lying triplet states.

In the present study, we wish to report our new *ab initio* calculations on the detailed mechanism *after*  $S_1/T_3$  transition. Additional non-adiabatic process is expected because  $T_3$  adiabatically connects to the  $H + C_2H(A\ ^2\Pi)$  limit, and therefore with a  $\sim 5.7\text{eV}$  photon energy,  $C_2H_2$  cannot dissociate directly on the  $T_3$  surface. A global schematic potential energy surface for the  $C_2H_2$  photodissociation from the  $S_1$  state has been obtained. The findings are summarized as the following.

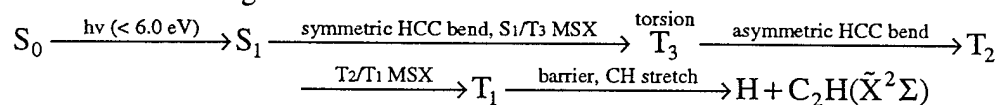
(i). The minima on the seam of crossing between  $S_1$  and  $T_3$  states are located in  $C_2$  symmetry, at 5.7eV above the  $S_0$  equilibrium. The symmetric H-C-C bending  $v_3$  is the critical degree of freedom for  $S_1/T_3$  crossing, and the MSX requires approximately (2-3) vibrational quanta in  $v_3$  on  $S_1$ . This is in close agreement with the recent experimental observation.

(ii). At a low photon energy, the molecule cannot dissociate on  $T_3$ . Due to the strong interaction between  $T_2$  and  $T_3$  when the H-C-C-H torsion angle is around  $90.0^\circ$ , no minimum exists on  $T_3$ . Starting from the  $S_1/T_3$  MSX,  $C_2H_2$  would easily reach  $T_{3-C_2}$ , a TS for adiabatic passage to  $T_2$ , and via asymmetric bending motion travel onto the second triplet state  $T_2$ .

(iii). At a low photon energy, the molecule cannot dissociate directly on  $T_2$  due to the presence of a high barrier. After coming to  $T_2$ ,  $C_2H_2$  will isomerize via asymmetric bending between *cis*- and *trans*- isomers on  $T_2$  and eventually hops to  $T_1$  around the *trans*- isomer when both H-C-C angles are compressed.

(iv). On the  $T_1$  surface, the molecule can finally dissociate by overcoming a late barrier. The reverse barrier height measured from dissociation limit is calculated to be  $992\text{cm}^{-1}$ , in agreement with the experimentally proposed value of  $560\text{cm}^{-1}$ .

(v). As a short summary, the entire photodissociation path at the photon energy of 6 eV or less can be described as the following.



This entire path involves an intersystem crossing from a singlet to a triplet as well as a nonadiabatic transition between two triplets. The promoting mode for these processes changes from the symmetric H-C-C bending to the H-C-C-H torsion, then to the H-C-C asymmetric bend and finally to the C-H stretch. The energy has to flow from one mode to the others before the next step can occur. Therefore, this process is expected to be very slow and inefficient. However, if there is no other channel for dissipation of the excitation energy, this dissociation can eventually take place. Finally, as found in our previous work,  $S_1$  and  $T_1$  do cross at the energy  $\sim 5.9\text{eV}$ , but with a much smaller  $H^{SO} \sim 1.6\text{cm}^{-1}$ . However, no additional non-adiabatic process is required after the  $S_1/T_1$  crossing, therefore the  $S_1/T_1$  direct crossing path can be competitive at the photon energy  $\sim 6\text{eV}$ .

### C-8. Potential Energy Surfaces for Photodissociation of $C_2H \rightarrow C_2 + H$ .

In a recent experiment of Y. -C. Hsu et al. (W. -C. Chiang, and Y. -C. Hsu, private communication) rovibronically (N, K-) resolved lifetimes of three vibrational levels of the B state of CCH radical were measured in a supersonic molecular beam. Considerable shorter lifetimes were observed at higher vibrational levels than level T (the assumed B origin), which was interpreted to be predissociation by coupling with X or A levels of CCH via C-type Coriolis interaction. Assuming no barrier exists in the dissociation process of the X and A states, an upper bound of  $D_0^0(\text{CC-H})$  was determined to be  $39388 \pm 7 \text{ cm}^{-1}$  (112.62 kcal/mol). Another interesting quantity that has been investigated by a number of authors is the branching ration of the photodissociation process. In the recent experiments of Jackson et al. (O. Sorkhabi, V. M. Blunt, H. Lin, D. Xu, J. Wrobel, R. Price, and W. M. Jackson, J. Chem. Phys. submitted) spectroscopic resolution is achieved by using laser induced fluorescence (LIF) to analyze the relative population of the photofragments in different electronic states. In this experiment, acetylene was used as the precursor for  $C_2H$  and was first photolyzed at 193nm. The photodissociation products  $C_2H(X^2\Sigma^+)$  and  $C_2H(A^2\Pi)$  absorb the photon of the same energy, undergo secondary photodissociation process which at 193nm can produces the  $C_2$  fragment in the following electronic states:  $X^1\Sigma_g^+$ ,  $A^1\Pi_u$ ,  $B^1\Delta_g$ ,  $B'^1\Sigma_g^+$ ,  $a^3\Pi_u$  and  $b^3\Sigma_g^-$ . The nascent population ratio of  $C_2$  in the X:A:B' electronic states was found to be 1:19:1.4. Clearly, non-adiabatic effect has to be involved to produce the ground state  $C_2$  product.

To further understand the experimental results of Hsu et al. and that of Jackson et al., high level *ab initio* calculations have been carried out to study seven electronic states of  $C_2H$ . The calculated equilibrium structure, energetics and vibrational frequencies for the  $3^2A'$  state at the CASPT2/PVTZ level are in good agreement with those obtained experimentally by Hsu et al. The transition dipole moments from the ground state  $C_2H$  to electronic excited states depend sensitively on the H-C-C bending angle and often peak at non-linear configurations. Based on this and the dissociation behavior of the excited states, we predict  $A^1\Pi_u$  and  $c^3\Sigma_u^+$   $C_2$  fragments to be rich in population, the former of which is experimentally detected recently by Jackson et al. The ground  $X^1\Sigma_g^+$  and the  $a^3\Pi_u$  state  $C_2$  are expected to be formed via the non-adiabatic process  $3^2A' \rightarrow 2^2A'$  or  $4^2A' \rightarrow 3^2A' \rightarrow 2^2A'$ , which is in accord with the experimentally observed lifetime pattern by Hsu et al. No reverse barrier for CC-H dissociation was found on the X and A electronic states of  $C_2H$  in the linear configuration. The  $2^2A'$  state, however, develops a distinct "barrier" (not a true saddle point) along dissociation coordinate when the H-C-C is significantly bent, due to the interaction with upper electronic state. Since the  $2^2A'$  state energetically prefers a linear dissociation, we suspect that the upper bound of the CC-H bond energy measured by Hsu et al. is not severally affected by this "barrier".

### C-9. Photodissociation of Ozone Anion.

The recent experimental work on  $O_3^-$  by Continetti (M. C. Garner, C. R. Sherwood, K. A. Hanold, R.

E. Continetti, Chem. Phys. Lett. 248, 20 (1996)) is interesting and puzzling. With two sources of  $O_3^-$ , they observed products in very different final states. Production of  $O_3^-$  by electron impact on  $O_2$  yields a vibrationally resolved kinetics energy release channel. Production of  $O_3^-$  by electron impact on  $O_3$ , on the other hand, produces  $O + O_2$  with no resolvable vibrational excitation, and 0.35eV larger maximum kinetics release. Larger rotational excitation of the products in the latter channel lead the experimentalists believe the existence of a bent excited state of  $O_3^-$ .

We have carried out CASSCF and CASPT2 calculations on the system. We found that the  $^2B_2$  excited state (which is bound) is rather bent, with an bond angle of  $90^\circ$  vs.  $116^\circ$  in the  $^2B_1$  ground state. At the ground state minima, a 2.37eV photon used in the experiment will excite the molecule to  $^2A_2$  state, which is repulsive along O-O stretch. Meta-IRC calculations clearly show that the initial motion of the molecule on the  $^2A_2$  surface is symmetric O-O stretch, which will lead to vibrationally excited  $O_2$ . At the  $^2B_2$  excited state minimum, the photon will excite the molecule to  $^2A_1$  state, which is also dissociative along O-O stretch. However, the minimum in  $C_{2v}$  symmetry has similar bond length as  $^2B_2$ , but a much opened O-O-O angle ( $120^\circ$  vs.  $90^\circ$ ). Meta-IRC calculations show that the initial motion of  $O_3^-$  on  $^2A_1$  is O-O-O bending, with little O-O stretch. Obviously, this will lead to more rotationally excited, less vibrationally excited products. The relative energetics also support a larger maximum kinetics energy release.

Further work would include the construction of a 3-D surface for the system and dynamic calculations on the photodissociation. As the first step, we have taken a model that includes three  $^2A''$  states. We neglect the interaction between the  $A''$  states and  $A'$  states, because for triatomic molecules, they are coupled only through the Coriolis coupling, which is usually weak. We have also neglected the interaction from the quartet states, which seems to be reasonable for light atoms like oxygen. We have scanned  $\sim 400$  points on the three potential energy surfaces, with CASSCF-MRCI/DZP(+) method. The second and third state undergoes an avoided crossing when the dissociating O-O distance is  $\sim 1.90\text{\AA}$ . In order to fit the potential energy surfaces into analytical functions, we need to transform the adiabatic states into diabatic ones. We did so by transforming the first diabatic state to be bright, and the second diabatic state to be dark. Afterwards, we fit the ground state and the two diabatic state surfaces into the well-known Murrell-Sorbie many body expansion function form. The fitting results are rather good, with the RMS error of the fitting  $\sim 0.02\text{-}0.04\text{eV}$ . The diabatic potential and the diabatic transition dipole moments between the ground electronic state to the first diabatic excited state have also been fitted into analytic functional form. Several cuts of the potential energy surfaces have been included.

## C-10. The Potential Energy Surface for Photodissociation of Triplet Ketene.

Determination and understanding of the detailed reaction mechanism and rate constant of reactions involving ketene have been the goal of numerous experimental as well as theoretical studies. Recently, much attention has been focused on the photodissociation of ketene into the triplet  $CH_2 + CO$ . Kim, Lovejoy and Moore (S. K. Kim, E. R. Lovejoy, and C. B. Moore, J. Chem. Phys. 102, 3202 (1995)) prepared rotational cold ketene on the  $S_0$  ground state ( $X^1A_1$ ) and used a UV laser to excite the molecule to the  $S_1$  singlet excited state ( $A^1A_2$ ), which then underwent intersystem crossing to the  $T_1$  triplet surface. The products,  $CH_2$  ( $^3B_1$ ) + CO, were detected using LIF of the CO fragment. At the first glance, the observed rate constants are very close to the prediction of the standard RRKM theory, and the energy dependence of the rate seems to exhibit a sharp stair function structure. However, upon closer inspection, they found that not all of the detailed fine structures in the rate constant could be explained using the standard RRKM.

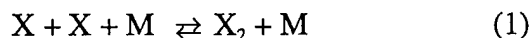
Gezelter and Miller (J. D. Gezelter and W. H. Miller, J. Chem. Phys. 104, 3553 (1996)) recently carried out reduced-dimension quantum calculations (1D and 2D ABC-DVR) for the microcanonical rate constant, trying to solve this mystery. Even though the overall results agreed with experimental findings, the step function structure was washed out by tunneling through the thin barrier predicted by Allen and Schaefer (W. D. Allen and H. F. Schaefer III, J. Chem. Phys. 89, 329 (1988)) with *ab initio* calculations. To explain the discrepancies, they have proposed that either the magnitude of the *ab initio* imaginary frequency ( $379i\text{ cm}^{-1}$  at the CCSD/TZ(2df,2p) level) is four times too large, or the  $S_0/T_1$  interaction might play some role in the transition state region.

To further clarify the reason behind those stair structures and the effect of intersystem crossings during the photodissociation, *ab initio* calculations have been carried out on potential energy surfaces for the photodissociation of ketene.  $S_0$  and  $S_1$  state cross extensively around the F-C region upon C-C-O bending,

and the  $S_1 \rightarrow S_0$  internal conversion is expected to be very efficient.  $S_1$  and  $T_1$  stay close in energy in the F-C region, but do not couple strongly due to the small spin-orbit coupling, and the direct  $S_1 \rightarrow T_1$  intersystem crossing is unlikely. The triplet state which produces the ground state products is likely to be formed via the process  $S_1 \rightarrow S_0 \rightarrow T_n$ .  $S_0$  crosses with the lowest triplet state ( $T_1$  or  $T_2$ ) at rather low energy near the triplet minimum. The  $S_0/T_n$  crossing persists all along the C-C dissociation pathway. As C-C is stretched, the energy of crossing increases and the crossing structure deviates substantially from the reaction path. These results suggest that, if intersystem crossing at higher potential energy is favored, the rate of reaction may reflect the dynamics of intersystem crossing and that on the triplet surface. The schematic photodissociation profile has been determined.

### C-11. Ab initio Molecular Orbital Study of the Trichlorine Radical, $Cl_3$ .

Trihalogens have been of interest to kineticists since the early sixties. These radicals represent fundamental recombination reactions which can be conducted in gas phase at room temperature as well as in solid phase at much colder temperatures, 10-20 K. The recombination reaction of a halogen is written conventionally as:



where M is the wall. Unusually high efficiency of this reaction was first observed by Davidson with



with  $X_2$  playing the role of the wall. Thus, a stable trihalogen compound must exist at room temperature. Recent experiments on  $X=Cl$  include those by Kawasaki et al. (M. Kawasaki, H. Sato and G. Inoue, J. Phys. Chem. 93, 7571 (1989)) and Lawrence et al. (W. G. Lawrence, R. M. Fulghum, and M. C. Heaven, J. Phys. Chem. 100, 18702 (1996)). These studies have established a long lived excited state resulting from microwave discharge excitations and photo excitations of mixtures containing  $Cl_2$  in the ground electronic state. No definite assignment has been given to the intense band in the blue region of the emission spectrum, but insinuations have been made that the band belongs to  $Cl_3$ .

Therefore, in collaboration with Dr. Mike Heaven, an experimental colleague at Emory who is supported by an AFOSR grant, we have performed ab initio calculations at CASSCF, CASPT2 and MRSDCI levels of theory, in order to clarify the ground and low-lying excited-state potential energy surfaces (PESs) of the  $Cl_3$  radical. The ground state has two  $Cl_2 \cdot Cl$  van der Waals complexes **L** and **B**. The linear asymmetric minimum **L** is in  ${}^2\Pi$ , with the Cl-Cl distance  $r = 3.90$  bohr, and the Cl-M (M: the  $Cl_2$  center-of-mass) distance  $R = 8.47$  bohr. The bent asymmetric minimum **B** is  ${}^2A'$ , with  $r = 3.90$  bohr,  $R = 6.85$  bohr and the angle between  $r$  and  $R$ ,  $\gamma = 66.5^\circ$ . Spin-orbit CI predicts that the global minimum is the linear **L** ( ${}^2\Pi_{3/2}$ ) with  $D_e(Cl_2(X)-Cl)$  of  $280\text{ cm}^{-1}$ . Low-lying doublet excited states have only one strongly bound structure, a linear symmetric **XLS** ( $1\text{ }{}^2\Pi_u$ ) with the bond distances of  $4.67$  bohr. This minimum, about  $9,000\text{ cm}^{-1}$  above the van der Waals minimum **L** and with a strong transition dipole moment with the ground  $X\text{ }{}^2\Pi_u$  state, is bound by approximately  $5,000\text{ cm}^{-1}$  with respect to  $Cl_2({}^3\Pi_u) + Cl$  asymptote. The quartet states have two minima, **QD3H** ( $1\text{ }{}^4A_1'$ ) in  $D_{3h}$  ( $r = 4.92$  bohr) about  $17,000\text{ cm}^{-1}$  above **L**, and **QD2H** ( $1\text{ }{}^4A''$ ) in  $C_{2v}$  ( $r_1 = 4.83$  bohr and  $\theta = 101.7^\circ$ ) about  $22,000\text{ cm}^{-1}$  above **L**. The present results do not support the on-going hypothesis of a long-lived ground state intermediate formed by the reaction:  $Cl_2 + Cl \rightarrow Cl_3$ , or give no evidence that  $Cl_3$  is responsible to a  $470\text{ nm}$  long-lived laser-induced fluorescence observed after isolating Cl and  $Cl_2$  in Ar matrix.

### C-12. The Potential Energy Surface for Photodissociation of Vinyloxy Radical.

In a series of papers including the latest (D. L. Osborn, H. Choi, D. H. Mordant, R. T. Bise, D. M. Neumark, and C. M. Rohfling, J. Chem. Phys. 106, 3049 (1997)), Neumark et al. have experimentally studied the photodissociation of the  $CH_2CHO$  radical, including the channels leading to  $CH_3+CO$  (Channel 1) and  $CH_2CO+H$  (Channel 2) products. The problems we are interested in are: a) the dissociation pathways for Channels 1 and 2 on  $X\text{ }{}^2A''$  and  $A\text{ }{}^2A'$  electronic surfaces; b) the explanation of the ratio between channels 1 and 2; c) the mechanisms of the internal conversion of a molecule in  $B\text{ }{}^2A''$  state to either X or A states.

We investigated in details the channel 2 (CH bond breaking)  $C_s$  and  $C_1$  pathways, with particular attention paid to the crossing between  $X\text{ }{}^2A''$  and  $A\text{ }{}^2A'$  states. We used (7e/6o)CASSCF/DZP method with further CASPT2 energy refining. The  $C_s$  seam of crossing (in the region of stretched CH bond) has been

found to occur in very low energy, leaving therefore a possibility for a molecule in X state to dissociate on the A surface through a low lying crossing. The planar ( $C_s$ ) TS4 on the  $A^2A''$  surface described by Osborn et al. was found in reality to be a second-order saddle point, with one  $A''$  imaginary frequency. It appears that TS5 described by Osborn et al. is the only true TS on the  $A^2A''$  Channel 2 pathway. However, they did not characterize this TS5 by an *ab initio* method but used parameters estimated using empirical rules for RRKM calculations, which reproduced accurately the experimental channel 2 vs 1 branching ratio of 4:1. Nevertheless, our calculations suggest that they underestimated the reverse barrier corresponding to the TS5 by about 0.3 eV, which should influence substantially the results of their RRKM calculations and making the explanation of the branching ratio open to question. The difficulty of the Osborn calculation has been traced to a small (5e/5o) active space used.

The question of the mechanism of the internal conversion remains the most difficult problem so far. The minimum on the seam of crossing (MSX) between  $X^2A''$  and  $A^2A'$  states has been located. However, it is still unclear how a molecule reaches the A state after being excited to the  $B^2A''$  state. MSX calculation (within  $C_s$  symmetry framework) do not produce any reasonable result. The suggested mechanism (M. Yamaguchi, Chem. Phys. Lett. 221, 531 (1994)) of coupling of B and A states by rotation of  $CH_2$  group about CC axes was investigated. Also numerous scans along the  $CH_2$  rotation coordinates have been performed. The two states really come close enough, and several minimum energy avoided crossing points have been located. However, all of them lie too high in energy, giving therefore no reasonable explanation for the  $1400\text{ cm}^{-1}$  value of the energy excess leading to the fluorescence quenching. Further study is in progress in the search of more appropriate mechanism of B/A crossing.

### C-13. The Potential Energy Surface for Photodissociation of Bromoiodoalkanes.

The photodissociation of haloalkanes which contain two different carbon-halogen bonds has been studied by several experimental groups. The experiments probing the photodissociation of  $CH_2BrI$ , 1,2- $C_2F_4BrI$  and 1,3- $C_3H_6BrI$  investigate product channels resulting from excitation in the  $n(I) \rightarrow \sigma^*(C-I)$  and  $n(Br) \rightarrow \sigma^*(C-Br)$  absorption bands, competition between several dissociation channels are observed in excitation of the  $n(Br) \rightarrow \sigma^*(C-Br)$  band. We study the mechanism of photodissociation of bromoiodomethane, 1-bromo-2-iodoethane and 1-bromo-3-iodopropane within the first two UV absorption bands with *ab initio* molecular orbital calculations. The adiabatic potential energy surfaces (PESs) of the ground electronic state and the low-lying excited states involved in the dissociation are explored by sa-CASSCF and CASPT2 methods along the C-Br and C-I bond coordinates. The calculated vertical excitation energies for  $n \rightarrow \sigma^*$  transitions are in good agreement with experiments. A seam of avoided crossing between two adiabatic excited states which involved  $n(I) \rightarrow \sigma^*(C-I)$  and  $n(Br) \rightarrow \sigma^*(C-Br)$  excitations on the two dimensional PESs is found. The excited adiabatic surfaces are diabitized, and the off-diagonal coupling between the diabetic states is evaluated. Based on the PESs, we propose a photodissociation mechanism which involves both adiabatic and diabatic processes to explain the different dissociation channels following excitation in the  $n(Br) \rightarrow \sigma^*(C-Br)$  band in the three systems. Calculations on the nonadiabatic transition probability by using Landau-Zener model do not agree with the experimental branching ratios and we need to find a more suitable model to calculate the nonadiabatic transition probability.

We also performed spin-orbit calculations on the bromoiodomethane and 1-bromo-2-iodoethane systems. PESs along C-Br bond coordinate for seventeen spin states resulting from the nine spin free states involved in the dissociation are explored. Calculations on the spin states eigenvectors and transition dipole moments showed that the initial excitation in the Franck-Condon region is not affected by spin-orbit coupling, but the dissociation processes including non-adiabatic transitions may be affected by spin-orbit coupling.

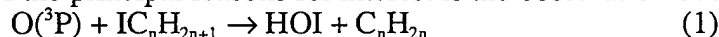
## D. Reactions and Dynamics in the Ground State.

### D-1. Anion Catalyzed Reaction of HOCl with HCl.

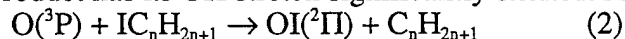
The reaction of  $HOCl + HCl \rightarrow Cl_2 + H_2O$  in the presence of chloride ion  $Cl^-$  has been studied at CCSD(T) and MP2 levels. The overall exothermicity is 15.5 kcal/mol, and the reaction has a high activation barrier of 46.5 kcal/mol.  $Cl^-$  is found to catalyze the reaction via the formation of  $HOCl \cdot Cl^-$ ,  $ClH \cdot HOCl \cdot Cl^-$  and  $Cl^- \cdot H_2O$  intermediate ion-molecule complexes or by interacting with a concerted four-center transition state of the reaction  $HOCl + HCl$ .

### D-2. The reaction $C_2H_5I + O \rightarrow HOI + C_2H_4$ .

Recently, a number of experiments have investigated the reactions of oxygen atoms with alkyl iodides. One of the principal reasons for interest is the observation of the spin-forbidden reaction channel:



in which the reaction begins in a triplet and produces products in the singlet. The work of Leone et al. shows that the HOI product has its OH stretch significantly excited. A spin-allowed channel:



have been studied by Grice et al. The spin-allowed channel is typically favored over the spin-forbidden channel, with branching ratios varied from 1.6 to 3, with the relative yield of OI increased at higher energies. These results have been interpreted that OI products are formed by two pathways, one of which is open at low impact energies and the other which opens at higher energies with a threshold of 8.6 kcal/mol.

We have studied the singlet and triplet potential energy surfaces for reactive collisions of  $O(^3P)$  and  $C_2H_5I$ . The resultant potential energy surfaces indicate that HOI is formed via a triplet complex and through a triplet/singlet intersystem crossing, followed by passage through a singlet intermediate and transition state for the intramolecular abstraction of  $\beta$ -hydrogen. All the relevant structures for this pathway are lower in energy than the reactants, and this pathway is accessible even at low impact energies. The calculations also indicate that OI may be formed by two channels. One is the same to the above singlet pathway up to the singlet intermediate, which now dissociates endothermically without barrier to give the products. The second channel is the direct dissociation of the triplet intermediate, and is open only when an enough excess energy to surmount a triplet transition state is provided. The product energy distribution is also discussed based on the structures of transition states.

### D-3. The Spin-forbidden Reaction $CH(^2\Pi) + N_2 \rightarrow HCN + N(^4S)$ Revisited.

**I. Ab initio Study on the Potential Energy Surfaces.** This reaction has fundamental importance in combustion chemistry, and its peculiar kinetics has attracts numerous experimental studies as well as theoretical calculations. The coexistence of spin-forbidden process and relatively deep potential well also attract interests from the quantum dynamics society. Quite recently, T. Seideman has carried out quantum mechanical calculation of the rate constant of the reaction using a 2 dimensional model potential energy surface. Even though some salient feature has been abstracted in this reduced dimensional study, a more careful study is definitely required for a reaction with complicated potential energy surface.

High level *ab initio* electronic structure theories have been applied to investigate the detailed reaction mechanism of the spin-forbidden reaction of  $CH(^2\Pi) + N_2 \rightarrow HCN + N(^4S)$ . The G2M(RCC) calculations provide accurate energetics for the intermediates and transition states involved in the reaction, whereas the B3LYP/6-311G(d,p) method overestimates the stability of some intermediates as much as ~10kcal/mol. A few new structures have been found on both the doublet and quartet electronic states, which are mainly involved in the dative pathways. However, due to the higher energies of these structures, the dominant mechanism remains to be the  $C_{2v}$  intersystem crossing mechanism. The  $C_{2v}$  MSX structures and the spin-orbit coupling between the doublet and quartet electronic states are rather close to those found in previous studies. Vibrational frequencies orthogonal to the norm of the seam have been calculated at the MSX from the first principle, which have been applied in a separate publication to calculate the rate of the titled reaction with a newly proposed non-adiabatic transition state theory for spin-forbidden reactions.

**II. Non-adiabatic Transition State Theory and Application.** The transition state theory (TST) has been extended straightforwardly to treat non-adiabatic processes and applied to study the rate constant of the spin-forbidden reaction  $CH(^2\Pi) + N_2 \rightarrow HCN + N(^4S)$ . A one-dimensional model was set up to calculate the intersystem crossing probability with the distorted wave approximation. The effect of orthogonal degrees of freedom was then considered by energy convolution with the vibrational frequencies orthogonal to the crossing seam at the minimum of the seam of crossing (MSX) obtained from the molecular orbital calculations. An expression for the cumulative reaction probability,  $N(E)$ , of the reaction was obtained by a straightforward extension of the unified statistical theory, where the MSX was treated as a transition state. The results of application of the non-adiabatic TST. The obtained  $N(E)$  seems to be consistent to that obtained by Seideman who used a Fermi-Golden-rule approach and 2-dimensional model potential surfaces. Nevertheless, the calculated thermal rate constant,  $k(T)$ , seems to be too low by two orders of magnitude



compared to experimental measurements and an empirical transition state study where empirical vibrational frequencies at the MSX are lower by a factor of two than those derived here. The disagreement strongly suggests that some important issues might have been overlooked. In particular, it may be a poor assumption that spin-forbidden transition takes place with uniform probability on the seam in the particular case we are considering.

#### **D-4. Highly Excited Vibrational States of HCP and Their analysis in Terms of Periodic Orbitals: The Genesis of Saddle-Node States and Their Spectroscopic Signature.**

We performed quantum mechanical bound-state calculations for HCP(X) state using an ab initio potential energy surface. The wave function of the first 700 states, corresponding to energies roughly 23000  $\text{cm}^{-1}$  above the ground vibrational state, are visually inspected and it is found that the majority can be uniquely assigned by three quantum numbers. The energy spectrum is governed, from the lowest excited states up to very high states, by a pronounced Fermi resonance between the CP stretching and the HCP bending mode leading to a clear polyad structure. At an energy of about 15000  $\text{cm}^{-1}$  above the origin, the states at the lowest end of the polyads rather suddenly change their bending character. While all states below this critical energy avoid the isomerization pathway, the states with the new behavior develop nodes along the minimum energy path and show large-amplitude motion with H swinging from the C- to the P-end of the diatomic entity. How this structural change can be understood in terms of periodic classical orbits and saddle-node bifurcations and how this transition evolves with increasing energy is the focal point of this research. The two different types of bending motion are clearly reflected by the rotational constants. The relationship of our results with recent spectroscopic experiments is discussed.

#### **D-5. Reactions of Hydrocarbon Radicals. The $\text{C}_6\text{H}_5 + \text{H}_2$ reaction system.**

The potential energy surface for the  $\text{C}_6\text{H}_5 + \text{H}_2$  reaction system has been calculated with the G2M(rcc,MP2) method. The system includes the reactions and  $\text{C}_6\text{H}_5 + \text{H}_2 \rightleftharpoons \text{C}_6\text{H}_6 + \text{H}$  (1) and  $\text{C}_6\text{H}_6 + \text{H} \rightleftharpoons \text{C}_6\text{H}_7$  (2). For the direct abstraction reaction(1), the barrier was found to be 8.8 kcal/mol, with the tunneling corrected TST rate constant  $k_1 = 9.48 \times 10^{-20} T^{2.43} \exp(-3159/T) \text{ cm}^3 \text{ molecule}^{-1} \text{ s}^{-1}$  covering 300-5000K. This result is consistent with the scattered kinetic data available in the literature. For addition reaction(2), the barrier was found to be 8.9 kcal/mol. The rate constant calculated solving the master equation, with the tunneling correction based on the RRRKM theory, gave  $k_1 = 5.27 \times 10^{-11} \exp(-1605/T) \text{ cm}^3 \text{ molecule}^{-1} \text{ s}^{-1}$  at the high-pressure limit and  $300 < T < 1000\text{K}$ . In this temperature regime, where most addition kinetics have been measured, the calculated results between 1 and 100 Torr encompass all experimental data. The rate constant  $k_2$  was found to be strongly pressure dependent above the room temperature. Additionally the effects of isotope substitution and possible secondary reactions on reported experimental data have been reported.

#### **D-6. Reactions of Nitrogen-Containing Radicals. Ab initio MO and TST calculations for the Rate Constant of the $\text{HNO} + \text{NO}_2 \rightarrow \text{HONO} + \text{NO}$ Reaction.**

Potential energy surfaces for various channels of the  $\text{HNO} + \text{NO}_2$  reaction have been studied at the G2M(RCC,MP2) level. The calculations show that direct hydrogen abstraction leading to the  $\text{NO} + \text{cis-HONO}$  products should be the most significant reaction mechanism. Based on TST calculations of the rate constant, this channel is predicted to have an activation energy of 6-7 kcal/mol and an A factor of  $\sim 10^{11} \text{ cm}^3 \text{ molecule}^{-1} \text{ s}^{-1}$  at ambient temperature. Direct H-abstraction giving  $\text{NO} + \text{trans-HONO}$  has a high barrier and the formation of *trans*-HONO would rather occur by the addition/1,3-H shift mechanism via the  $\text{HN(O)NO}_2$  intermediate or by the secondary isomerization of *cis*-HONO. The formation of  $\text{NO} + \text{HNO}_2$  can take place by direct hydrogen transfer with the barrier of  $\sim 3$  kcal/mol higher than that for  $\text{NO} + \text{cis-HONO}$  channel. The formation of  $\text{HNO}_2$  by oxygen abstraction is predicted to be the least significant reaction channel.

## Publications.

1. A. M. Mebel, K. Morokuma and M. C. Lin, *Ab Initio Molecular Orbital Study of Potential Energy Surface for the Reaction of  $C_2H_3$  with  $H_2$  and Related Reactions*, J. Chem. Phys., **103**, 3440-3449 (1995).
2. A. M. Mebel, C.-C. Hsu, M. C. Lin and K. Morokuma, *An Ab Initio Molecular Orbital Study of Potential Energy Surface of the  $NH_2 + NO_2$  Reaction*, J. Chem. Phys., **103**, 5640-5649 (1995).
3. A. M. Mebel, K. Morokuma and M. C. Lin, *Modification of the Gaussian-2 Theoretical Model: The Use of Coupled Cluster Energies, Density Functional Geometries and Frequencies*, J. Chem. Phys., **103**, 7414-7421 (1995).
4. Y. Amatatsu and K. Morokuma, *A Theoretical Study on the Photochemical Reaction of ICN in Liquid Ar*, Chem. Phys. Lett., **245**, 469-474 (1995).
5. K. M. Dunn and K. Morokuma, *Ab Initio Study of the Photochemical Dissociation of Methylamine*, J. Phys. Chem., **100**, 123-129 (1996).
6. A. M. Mebel and K. Morokuma, *Theoretical Study of the Reaction of HCl with  $ClONO_2$  catalyzed by  $NO_3^-$ . "Attachment-Detachment" Mechanism for the Anion-Catalyzed Neutral Reactions*. J. Phys. Chem., **100**, 2985-2992 (1996).
7. A.M. Mebel, E.W.G. Diau, M.C. Lin and K. Morokuma, *Theoretical Rate Constants for the  $NH_3+NO_x \rightarrow NH_2+HNO_x$  ( $x=1,2$ ) Reactions by Ab Initio MO/VTST Calculations*, J. Phys. Chem., **100**, 7517-7525 (1996).
8. R. Liu, K. Morokuma, A.M. Mebel and M.C. Lin, *Ab Initio Study of the Mechanism for the Thermal Decomposition of the Phenoxyl Radical*, J. Phys. Chem., **100**, 9314-9322 (1996).
9. Y. Amatatsu, S. Yabushita and K. Morokuma, *Full Nine-dimensional Ab Initio Potential Energy Surfaces and Trajectory Studies of A-band Photodissociation Dynamics:  $CH_3I^* \rightarrow CH_3+I$ ,  $CH_3+I^*$ , and  $CD_3I^* \rightarrow CD_3+I$ ,  $CD_3+I^*$* , J. Chem. Phys., **104**, 9783-9794 (1996).
10. S. C. Frantos, H.-M. Keller, R. Schinke, K. Yamashita and K. Morokuma, *Normal Mode and Isomerization Bending States in HCP: Periodic Orbit Assignment and Spectroscopic Signature.*, J. Chem. Phys., **104**, 10055-10058 (1996).
11. R. Liu, Q. Cui, K. Dunn and K. Morokuma, *Ab Initio Molecular Orbital Study of the Mechanism of Photodissociation of Trans-azomethane*, J. Chem. Phys., **105**, 2333-2345 (1996).
12. A. M. Mebel, M. C. Lin, K. Morokuma and C. F. Melius, *Theoretical Study of Reactions of  $N_2O$  with NO and OH Radicals*, Int. J. Chem. Kin., **28**, 693-703 (1996).
13. A. Luna, A. M. Mebel and K. Morokuma, *A Density Functional Study of the Global Potential Energy Surfaces of the  $[H,C,N,O]^+$  System in Doublet and Quartet States*, J. Chem. Phys., **105**, 3187-3205 (1996).
14. A. M. Mebel, E. W. G. Diau, M. C. Lin and K. Morokuma, *Ab Initio and RRKM Calculations for Multichannel Rate Constants of the  $C_2H_3 + O_2$  Reaction*, J. Am. Chem. Soc., **118**, 9759-9771 (1996).
15. A. M. Mebel, A. Luna, M. C. Lin and K. Morokuma, *Theoretical Study of the Global Potential Energy Surfaces of the  $[H,C,N,O]$  System in Singlet and Triplet States*, J. Chem. Phys., **105**, 6439-6454 (1996).
16. Q. Cui, K. Morokuma and J. F. Stanton, *Ab initio MO Studies on the Photodissociation of  $C_2H_2$  from the  $S_1$  ( $^1A_u$ ) State. Non-adiabatic Effects and S-T Interaction*, Chem. Phys. Lett., **263**, 46-53 (1996).
17. Q. Cui and K. Morokuma, *Ab initio MO Studies on the Photodissociation of the Methoxy Family  $CX_3Y$  ( $X=H, F$ ;  $Y=O, S$ ) from the  $\tilde{A}^2A_1$  State*, Chem. Phys. Lett., **263**, 54-62 (1996).

18. A. M. Mebel, M. C. Lin, T. Yu and K. Morokuma, *Theoretical Study of Potential Energy Surface and Thermal Rate Constants for the  $C_6H_5 + H_2$  and  $C_6H_6 + H$  Reactions*, J. Phys. Chem. A, **101**, 3189-3196 (1997).
19. S. L. Richardson, J. S. Francisco, A. M. Mebel and K. Morokuma, *Can Chlorine Anion Catalyze the Reaction of HOCl with HCl?*, Chem. Phys. Lett., **270**, 395-398 (1997).
20. Q. Cui and K. Morokuma, *Ab initio MO Studies on the Photodissociation of  $C_2H_2$  from the  $S_1$  ( $^1A_u$ ) State. II. Mechanism Involving Triplet States*, Chem. Phys. Lett., **272**, 319-327 (1997).
21. Q. Cui and K. Morokuma, *Ab initio Study of Non-adiabatic Interactions in the Photodissociation of Ketene*, J. Chem. Phys., **107**, 4951-4959 (1997).
22. C. Beck, H.-M. Keller, S. Y. Grenschchikov, R. Schinke, S. C. Farantos, K. Yamashita and K. Morokuma, *Highly excited vibrational states of HCP and their analysis in terms of periodic orbits: The genesis of saddle-node states and their spectroscopic signature*, J. Chem. Phys., **107**, 9818-9834 (1997).
23. Q. Cui and K. Morokuma, *Ab initio Studies on the Electronic Excited States of  $C_2H$* , J. Chem. Phys., **108**, 626-636 (1998).
24. J. E. Stevens, Q. Cui, and K. Morokuma, *An ab initio Study of the Dissociation of HNCO in the  $S_1$  Electronic State*, J. Chem. Phys., **108**, 1452-1458 (1998).
25. J. E. Stevens, Q. Cui and K. Morokuma, *An ab initio Investigation of Spin-allowed and Spin-forbidden Pathways of the Gas Phase Reactions of  $O(^3P) + C_2H_5I$* , J. Chem. Phys., **108**, 1544-1551 (1998).
26. A. L. Kaledin, M. C. Heaven, W. G. Lawrence, Q. Cui, J. E. Stevens and K. Morokuma, *Ab initio Molecular Orbital Study of the Trichlorine Radical,  $Cl_3$* , J. Chem. Phys., **108**, 2771-2783 (1998).
27. Q. Cui and K. Morokuma, *Ab initio study on the mechanism of  $C_2H_2^+ + NH_3$  reaction. — Efficient charge transfer and proton transfer processes competing with stable complex formation*. J. Chem. Phys., **108**, 4021-4030 (1998).
28. Q. Cui and K. Morokuma, *Ab initio studies on the electronic excited states and photodissociation of  $O_3$  anion*, J. Chem. Phys., **108**, 7684-7694 (1998).
29. A. L. Kaledin, M. C. Heaven, and K. Morokuma, *Ab initio Potential Energy Surfaces for the  $I(^2P_{3/2}) + O_2(a^1\Delta_g) \rightleftharpoons I(^2P_{1/2}) + O_2(X^3\Sigma_g^-)$  Energy Transfer Process*, Chem. Phys. Lett., **289**, 110-117 (1998).
30. Q. Cui, Z. Liu and K. Morokuma, *Theoretical study on the mechanism of  $CH_4 + C_2H_2^+$  reaction. Mode-enhancement effect*, J. Chem. Phys., **109**, 56-62 (1998).